

Photodynamic Inactivation of *Staphylococcus aureus* Biofilms Using a Hexanuclear Molybdenum Complex Embedded in Transparent polyHEMA Hydrogels

Noelia López-López, Ignacio Muñoz Resta, Rosa de Llanos, Juan F. Miravet, Maxim Mikhaylov, Maxim N. Sokolov, Sofía Ballesta, Isabel García-Luque,* and Francisco Galindo*

Cite This: *ACS Biomater. Sci. Eng.* 2020, 6, 6995–7003

Read Online

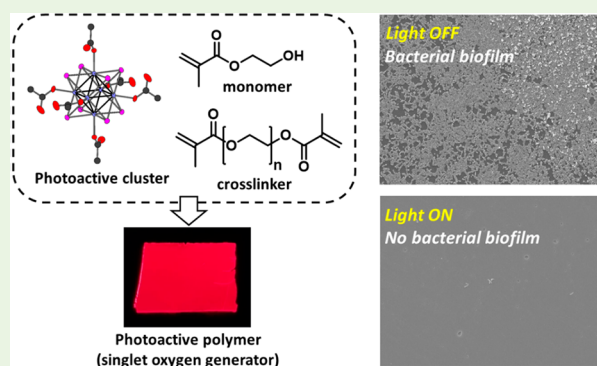
ACCESS |

Metrics & More

Article Recommendations

Supporting Information

ABSTRACT: Three new photoactive polymeric materials embedding a hexanuclear molybdenum cluster $(\text{Bu}_4\text{N})_2[\text{Mo}_6\text{I}_8(\text{CH}_3\text{COO})_6]$ (**1**) have been synthesized and characterized by means of Fourier-transform infrared spectroscopy (FTIR), thermogravimetric analysis (TGA), and emission spectroscopy. The materials are obtained in the format of transparent and thin sheets, and the formulations used to synthesize them are comprised of 2-hydroxyethyl methacrylate (HEMA), as a polymerizable monomer, and ethylene glycol dimethacrylate (EGDMA) or poly(ethylene glycol)dimethacrylate (PEGDMA), as cross-linkers. All the polymeric hydrogels generate singlet oxygen ($^1\text{O}_2$) upon irradiation with visible light (400–700 nm), as demonstrated by the reactivity toward two chemical traps of this reactive species (9,10-dimethylanthracene and 1,5-dihydroxynaphthalene). Some differences have been detected between the photoactive materials, probably attributable to variations in the permeability to solvent and oxygen. Notably, one of the materials resisted up to 10 cycles of photocatalytic oxygenation reactions of 1,5-dihydroxynaphthalene. All three of the polyHEMA hydrogels doped with **1** are efficient against *S. aureus* biofilms when irradiated with blue light (460 nm). The material made with the composition of 90% HEMA and 10% PEGDMA (**Mo6@polymer-III**) is especially easy to handle, because of its flexibility, and it achieves a notable level of bacterial population reduction ($3.0 \log_{10}$ CFU/cm²). The embedding of **1** in cross-linked polyHEMA sheets affords a protective environment to the photosensitizer against aqueous degradation while preserving the photochemical and photobactericidal activity.



INTRODUCTION

Antibiotic-resistant bacteria are a great menace for modern societies since uncontrolled spreading of such pathogens can lead to serious nosocomial infections, which imply an enormous economic burden for public health systems.¹ One of the most important features of many pathogenic microorganisms is their ability to form resistant biofilms, *i.e.*, organized macro-colonies of bacterial cells, which are much more difficult to eradicate than isolated bacteria in suspension.² It is considered that more than 60% of microbial infections are originated by biofilms grown in surfaces.³

Antimicrobial photodynamic inactivation (aPDI) of microorganisms like bacteria, fungi, and viruses is an attractive tool that has been recently employed to prevent the spreading and growth of microbial pathogens. This approach implies the use of a photosensitizer, which in combination with light leads to the generation of cytotoxic species like singlet oxygen ($^1\text{O}_2$) or superoxide ($\text{O}_2^{\bullet-}$).^{4–9} A great number of publications have appeared during the last years, advocating for the use of this strategy, with an emphasis in the development of materi-

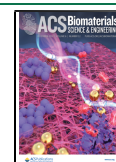
als,^{10–14} especially to be used for the manufacture of healthcare-related objects.^{15–17}

Currently there is a growing interest in developing new families of photosensitizers different from classical ones like Rose Bengal, methylene blue, or porphyrins/phthalocyanines, which are ubiquitously found in the literature and employed with great success in the past but are not exempt from drawbacks (photobleaching, tendency to aggregation, *etc.*).¹⁸ The group of hexanuclear molybdenum clusters described by the formula $[\text{Mo}_6\text{L}_8^i\text{L}_6^a]^{n-}$ (L^i and L^a are inner and apical ligands, respectively) has been receiving increasing attention due to their outstanding photophysical properties. A great number of such species have been described so far, both in

Received: July 5, 2020

Accepted: November 1, 2020

Published: November 19, 2020



solution^{19–29} and immobilized in a series of supports, such as polyurethane, poly(methyl methacrylate), zinc oxide, and other materials.^{30–43} After excitation with visible light, the triplet excited state is very efficiently populated, and many of such complexes, especially the iodides ($L = I$), are able to emit phosphorescence in the deep-red region of the spectrum, even at room temperature. Another relevant property of this class of complexes is their ability to generate 1O_2 after irradiation. This reactive oxygen species is known to have a great variety of applications, from oxygenation reactions^{44,45} to the aforementioned elimination of pathogenic microorganisms. In this last regard, the antibacterial applications of the $\{Mo_6\}$ clusters are still far from full development. Only a few cases of photobactericidal materials based on hexanuclear molybdenum clusters have been reported. We have shown that $(Bu_4N)_2[Mo_6I_8(CH_3COO)_6]$ (**1**) supported on macroporous and gel type cationic polystyrene is able to kill Gram-positive (*Staphylococcus aureus*) and Gram-negative (*Pseudomonas aeruginosa*) bacteria.^{46,47} Kirakci et al. have shown that irradiated complexes of $[Mo_6I_8(Ph_3P(CH_2)_4COO)_6]Br_4$ can reduce the population of Gram-positive *Enterococcus faecalis* and *S. aureus*.⁴⁸ Additionally, Vorotnikova et al. have shown that $(Bu_4N)_2[Mo_6I_8(CF_3(CF_2)_6COO)_6]$ used as an additive to polymer F-32L can kill *Escherichia coli*, *S. aureus*, *Salmonella typhimurium*, and *P. aeruginosa* upon irradiation.⁴⁹ It must be noted that all the above-mentioned investigations report bacteria in the planktonic state.

The purpose of this article is to present a series of polymeric hydrogel materials, in the format of thin polymeric films, embedding **1** as a photosensitizer capable of generating 1O_2 very efficiently upon irradiation and significantly suppressing the growth of *S. aureus* biofilms. To the best of our knowledge, this is the first example of use of a hexanuclear molybdenum cluster, in combination with light, to prevent the growth of a bacterial biofilm, specifically of *S. aureus*. We hope that these results will contribute to developing the field of aPDI, specifically against bacterial biofilms, and to expand the use of this new class of $\{Mo_6\}$ nanoclusters in healthcare materials, such as catheters, gloves, and thermometers, or in ordinary objects, such as computer keyboards, doorknobs, and mobile phone screens.

RESULTS AND DISCUSSION

Following our previously described procedures for the preparation of polymeric hydrogel sheets entrapping optically active molecules and nanoparticles,^{50–56} cluster **1** (1 wt %) was dissolved in three different formulations comprising monomer 2-hydroxyethylmethacrylate (HEMA) and two types of cross-linkers: ethylene glycol dimethacrylate (EGDMA) and poly(ethylene glycol)dimethacrylate (PEGDMA) (Figure 1). The aim of using different types and proportions of cross-linkers was to study the effect of these polymerizable components on the photodynamic performance of fabricated materials. According to our experience, the introduction of PEGDMA in a low percentage increases notably the permeability of the films to inorganic species such as nitrite. In Table 1, the three formulations employed for this study are shown. Polymers based on the monomer HEMA (leading to the so-called polyHEMA materials) have been described in the literature for years due to their high water permeability and biocompatibility. For instance, they form the basis of contact lenses, orthopedic implants, and drug delivery devices.^{57,58} Our aim was to develop matrixes strong enough to retain **1** but with

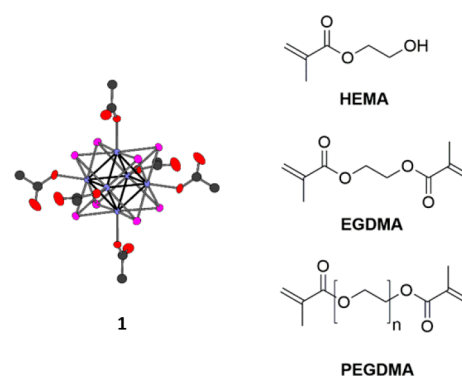


Figure 1. Structures of the octahedral cluster $(Bu_4N)_2[Mo_6I_8(CH_3COO)_6]$ (**1**), monomer HEMA, and cross-linkers EGDMA and PEGDMA. For **1**, the color code for the external ligands: red = oxygen, gray = carbon. Color code for the internal atoms: pink = iodide, blue = molybdenum.

enough permeability to allow O_2 to get in and 1O_2 to get out of the materials. The mixtures of olefins indicated in Table 1 (with added 1 wt % of azobisisobutyronitrile, AIBN) were introduced into glass molds (see previous procedures^{50–56}) and kept at 85 °C during 15 min. This procedure induces radical polymerization, leading to the formation of transparent films of polymeric hydrogels. After the mechanical removal of the molds, a series of polymeric films were obtained. The polymers embedding the $\{Mo_6\}$ cluster were named **Mo6@polymer-I**, **Mo6@polymer-II**, and **Mo6@polymer-III**, whereas the control materials without the photosensitizer were named simply **I**, **II**, and **III**. The materials were washed and characterized by means of Fourier-transform infrared spectroscopy (FTIR), thermogravimetric analyses (TGA), and emission spectroscopy. The thicknesses of the films were measured, giving the average value of $(120 \pm 10) \mu m$.

The infrared spectra of the samples showed the typical pattern of cross-linked polyHEMA materials, with a broad band around 3400 cm^{-1} corresponding to the O—H stretching, which impart hydrophilicity to the hydrogels. Also worth of note is the disappearance of vibration at 1640 cm^{-1} corresponding to the C=C bonds in the HEMA monomer and EGDMA or PEGDMA cross-linkers, as a result of the polymerization reaction. No band corresponding to the molybdenum complex was detected, due to its low concentration in the materials (see the spectra in the Supporting Information (SI) file). The samples were also analyzed by TGA, and interesting differences were found between the polyHEMA polymers containing a molybdenum cluster and the corresponding controls without the photosensitizer. As it can be seen in the SI file, all the six samples commonly displayed a loss of mass below 300 °C, corresponding to the decomposition of the polyHEMA structure (10% mass loss at about 250 °C; full decomposition at around 400 °C), but the samples containing the photosensitizer do not lose the full weight of the material until 500 °C (10% mass loss occurring at about 270–280 °C). This fact would point out to some kind of additional cross-linking effect of the molybdenum cluster on the structure of the materials, the study of which is out of the scope of this paper. Regarding the emission measurements, the samples under UV excitation emit a reddish phosphorescence observable even with the naked eye (see Figure S2), and the spectrum of such luminescence reveals the typical broad band of emissive

Table 1. Compositions of Monomer and Cross-Linker Mixtures Leading to the Polymers Used in This Study

	monomer (% wt)		cross-linkers (% wt)		photosensitizer
	HEMA	EGDMA	PEGDMA		I ^a
Mo6@polymer-I	67	33			yes
I	67	33			no
Mo6@polymer-II	90	10			yes
II	90	10			no
Mo6@polymer-III	90		10		yes
III	90		10		no

^a1 wt % relative to the total mass of monomer and cross-linker.

hexanuclear molybdenum complexes between 600 and 750 nm.^{19–43,46–49} Minor differences can be found between the polymeric samples and also when compared to a solid sample of **1** and to an ethanolic solution of the photosensitizer (see Figure 2), probably due to different solvation environments, in

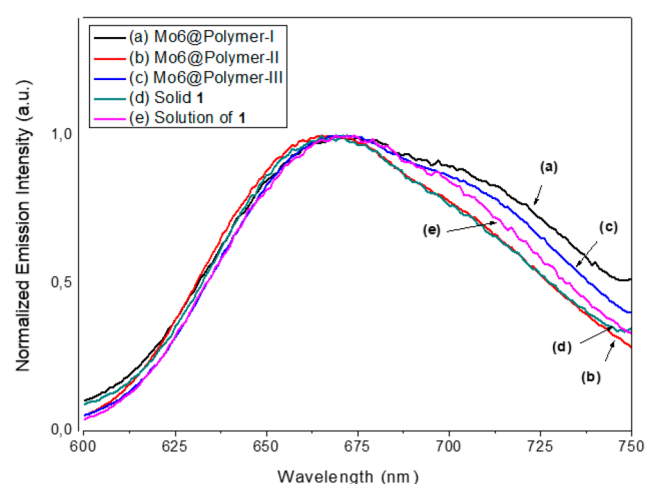


Figure 2. Normalized emission spectra of Mo6@polymer-I, Mo6@polymer-II, Mo6@polymer-III, **1** in ethanol solution and **1** in the solid state ($\lambda_{exc} = 470$ nm).

agreement with the literature.^{19–43,46–49} In the case of the materials here described, the presence of this emissive band confirms that the structural integrity of the photosensitizer remains intact after the polymerization reaction. Also, it could be speculated that, due to the low concentration of **1** and to the anionic nature of this photosensitizer, aggregation does not take place (future microscopic studies will shed light on the distribution of **1** within these and other polyHEMA matrixes).

Next, we proceeded to study the photochemical performance of the obtained polymeric hydrogels doped with **1**. The ability of the polymeric photosensitizers to generate ¹O₂ was checked by the means of two benchmark reactions: the transformation of 9,10-dimethylanthracene (DMA) into its endoperoxide (DMA·O₂) and the conversion of 1,5-dihydroxynaphthalene (DHN) into juglone. Both reactions can be followed easily by means of UV–vis spectroscopy, as can be seen in Figures 3 and 4.

The conversion of DMA after 90 min of irradiation with white light, attained with the three polymers under study, is very high (see Figure 5), being 83% for Mo6@polymer-I, 97% for Mo6@polymer-II, and 97% for Mo6@polymer-III. Also, control irradiations were conducted with empty matrixes, and conversions of around 10% were obtained. It must be noted that DMA is able to generate a small amount of ¹O₂ since

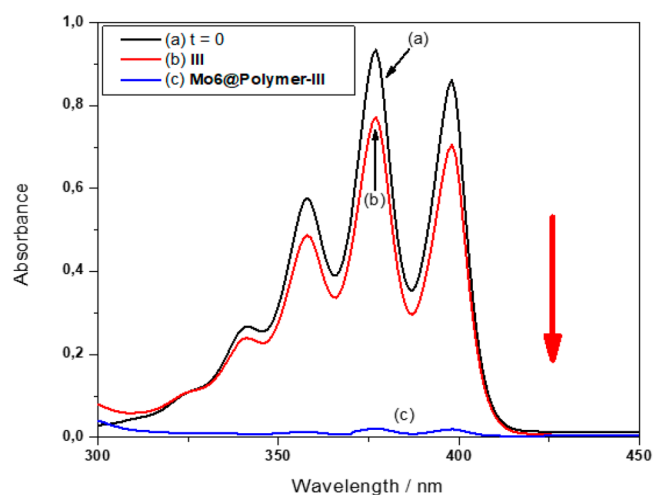
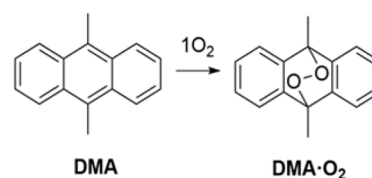


Figure 3. Up: reaction between DMA and ¹O₂. Bottom: representative example of such a reaction using Mo6@polymer-III as the supported photosensitizer and DMA (10^{−4} M) as the ¹O₂ trap in EtOH:H₂O (1:1). (a) Initial absorption of DMA, (b) absorption of DMA after irradiation for 90 min in the presence of III as control, and (c) absorption of DMA after irradiation for 90 min in the presence of Mo6@polymer-III. Light source: two white light LED lamps (11W each, 400–700 nm).

some residual light can be absorbed by this probe at ca. 400 nm. But, this self-oxidation process is much less important than the oxygenation reaction promoted by the clusters embedded on the polyHEMA films. Additionally, it must be indicated that no leaching of **1** was observed during the course of the experiments (lack of absorption or emission of the supernatant solutions after equilibration of films with solvent overnight).

The photoactivity was confirmed by the photo-oxidation of DHN to juglone, as can be seen in Figure 6 (again, some auto-oxidation of this substrate was observed, but the amount is minimal in comparison with the photoreactivity induced by the molybdenum cluster). Interestingly, the behaviors of the three materials under study are slightly different, with yields of juglone, after 120 min of irradiation, varying from 65% (Mo6@polymer-I) to 85% (Mo6@polymer-II) and 92% (Mo6@polymer-III). This trend might reflect the higher permeability of the hydrogel matrixes made with a higher amount of HEMA (90% of HEMA in Mo6@polymer-II and Mo6@polymer-III

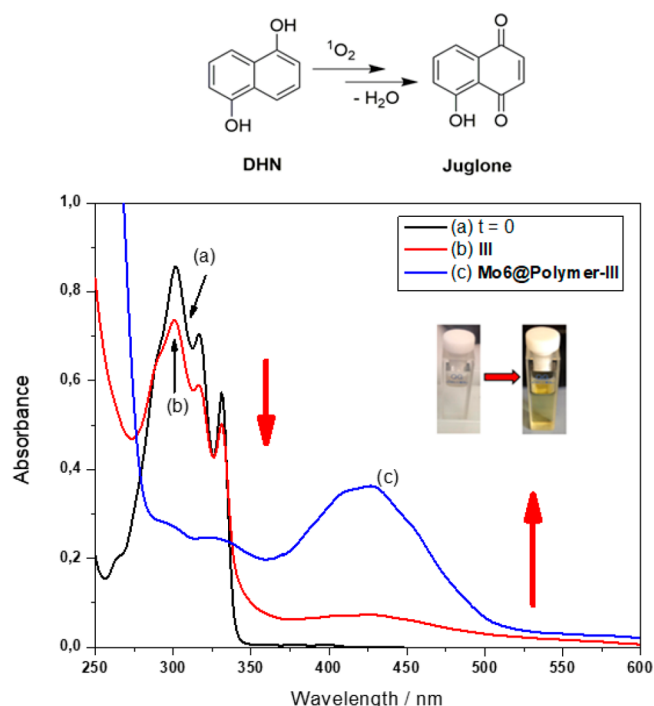


Figure 4. Up: reaction between DHN and $^1\text{O}_2$. Bottom: representative example of such reaction using Mo6@polymer-III as the supported photosensitizer and DHN (10^{-4} M) as the $^1\text{O}_2$ trap in DCM:MeOH (9:1). (a) Initial absorption of DHN, (b) absorption of DHN after irradiation for 120 min in the presence of control III, and (c) absorption of DHN after irradiation for 120 min in the presence of Mo6@polymer-III. Light source: two white light LED lamps (11W each, 400–700 nm).

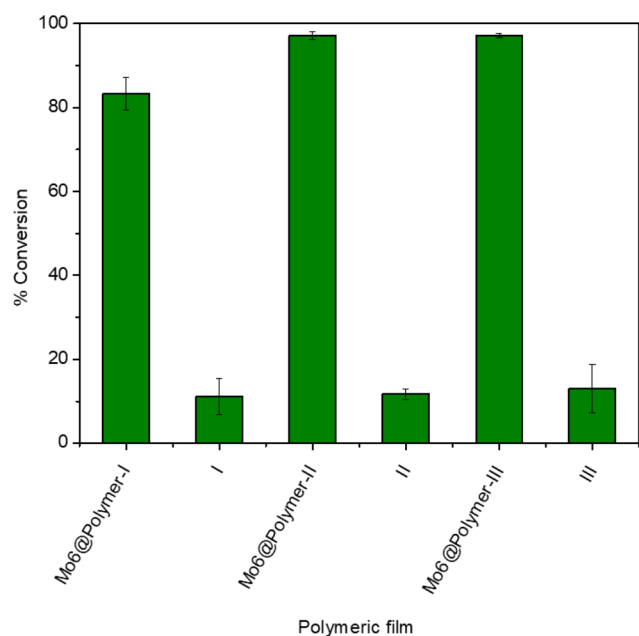


Figure 5. Conversions of DMA after reaction with $^1\text{O}_2$. Irradiation of polymers with white light in the presence of DMA (10^{-4} M in EtOH:H₂O, 1:1). Total irradiation time is 90 min.

vs 67% in Mo6@polymer-I), in agreement with previous reports from our group dealing with chromogenic and fluorogenic sensing materials.^{50–56} Especially notable is the influence of the cross-linker PEGDMA, used in the

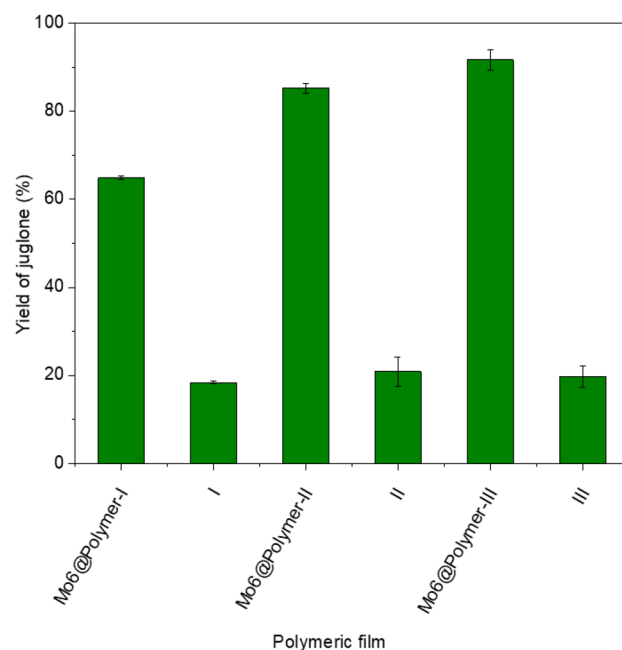


Figure 6. Yields of juglone in the reaction of DHN with $^1\text{O}_2$. Irradiation of polymers with white light in the presence of DHN (10^{-4} M in DCM:MeOH, 9:1). Total irradiation time is 120 min.

manufacture of Mo6@polymer-III, which is able to create a more flexible and permeable scaffold and, in consequence, to improve the photo-oxygenation efficiency of DHN.

One of the most valuable properties of complex 1, as earlier reported, is its high resistance to photobleaching under photochemical stress.^{46,47} In order to elucidate whether this property is conserved in the polyHEMA films, a sample of Mo6@polymer-III was submitted to several cycles of irradiation, using the conversion of DHN to juglone as test reaction. As shown in Figure 7, the photocatalytic ability of Mo6@polymer-III remarkably withstood 10 cycles of irradiation without important signs of fatigue. This issue is sometimes overlooked when developing materials for aPDI and this is a characteristic that should be studied, since the

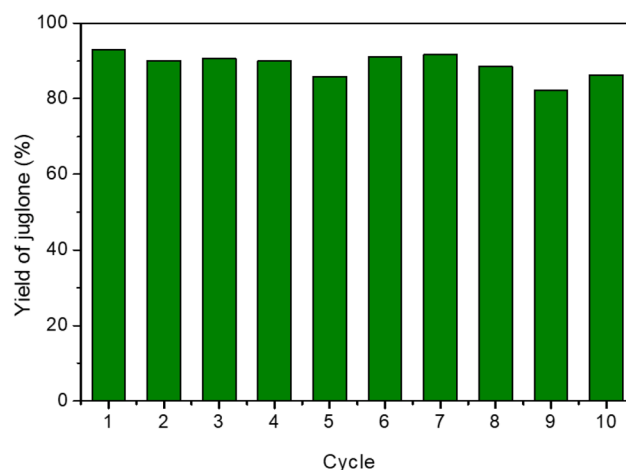


Figure 7. Yields of juglone in the reaction of DHN with $^1\text{O}_2$ during 10 cycles of irradiation. Irradiation of Mo6@polymer-III with white light in the presence of DHN (10^{-4} M in DCM:MeOH, 9:1). For each cycle, the irradiation time is 120 min.

materials with purported antimicrobial properties should also show endurance after prolonged times of exposure to light. These results are in agreement with the previously reported photoreactivity of **1** supported on polystyrene, for which no loss of activity was detected after repeated use in the photosensitized oxygenation of DMA.^{46,47}

Finally, the antimicrobial photodynamic activities of different polyHEMA hydrogels containing the {Mo₆} complexes against biofilms of *S. aureus* were evaluated (see Figures 8 and

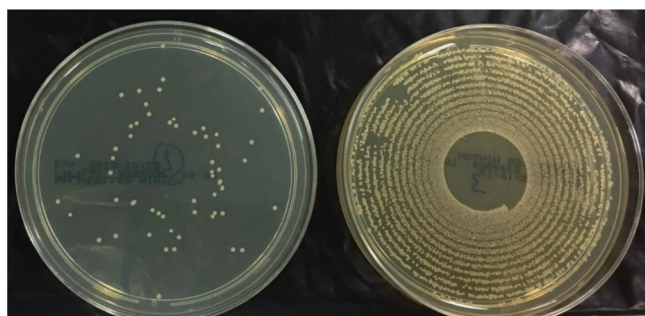


Figure 8. Representative visual example of bacteria growing in Mueller Hinton agar plates previously inoculated using a spiral plater. Left: polymeric film Mo6@polymer-III and light. Right: control without light (Mo6@polymer-III dark).

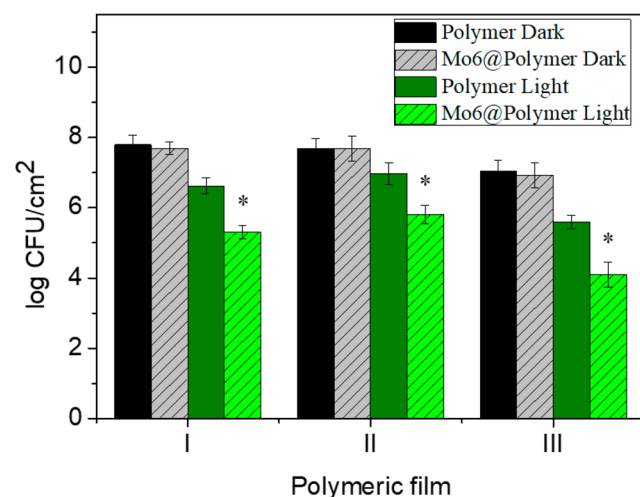


Figure 9. Antimicrobial photodynamic activity of different poly-HEMA matrixes containing {Mo₆} complexes against biofilms of *S. aureus* ($n = 3$). * $p < 0.05$.

9). All the polymeric films were studied in conditions of biofilm formation, and all showed antimicrobial activity, but some differences between these materials were found. The operational procedure followed to carry out this study is the following one: on small pieces of layers of Mo6@polymer-I, II, and III (and respective control materials without a photosensitizer), biofilms of *S. aureus* were allowed to grow (see the Experimental Section). Afterward, they were irradiated with blue light (460 nm) with a total fluence of 120 J/cm². Once finished with the irradiation period, the biofilms were detached from the surface and the survival of the bacteria was estimated by colony counting. We followed a well-established methodology employing conditions that ensure the formation of a

biofilm,⁵⁹ which has been used by part of us in the past with positive results.^{60–62} Regarding the quantification of the bacterial survival, the colony counting methodology has proven to be a very reliable methodology.⁶³

When comparing the studied polymers, the behavior of Mo6@polymer-III is especially remarkable, which caused a reduction of 3.0 log₁₀ CFU/cm² of the initial population of *S. aureus* (see in Figure 8, bacteria growing in Mueller Hinton agar plates corresponding to irradiated and nonirradiated samples of Mo6@polymer-III; and see in Figure 9, the complete set of assays for all the materials). This result is of merit, since it is considered that a treatment has effective bactericidal activity when the initial inoculum is reduced by 99.9% (i.e., 3.0 log₁₀ CFU/cm²).⁶⁴ A slightly lower reduction rate was achieved with Mo6@polymer-I (2.8 log₁₀ CFU/cm²), while Mo6@polymer-II showed a reduction of 1.9 log₁₀ CFU/cm². A practical question was also observed, which could have relevance for future studies; whereas materials Mo6@polymer-I and II were rigid and showed some tendency to break into pieces, the manipulation of Mo6@polymer-III was much easier due to its flexibility. Controls in the dark, both with and without **1**, showed no significant reduction of the initial population. Another interesting observation is that the polymers without a photosensitizer (controls I, II, and III) exposed to the light were able to reduce the population of *S. aureus* from about 1.0 to 1.5 log₁₀ CFU/cm², but this effect could be ascribed to the well-known bactericidal effect of blue light alone.⁶⁵

Additional measurements by scanning electron microscopy (SEM) confirmed the formation of *S. aureus* biofilms on the surface of the polyHEMA hydrogels and a striking reduction of such structures upon irradiation. Parts a and c of Figure 10

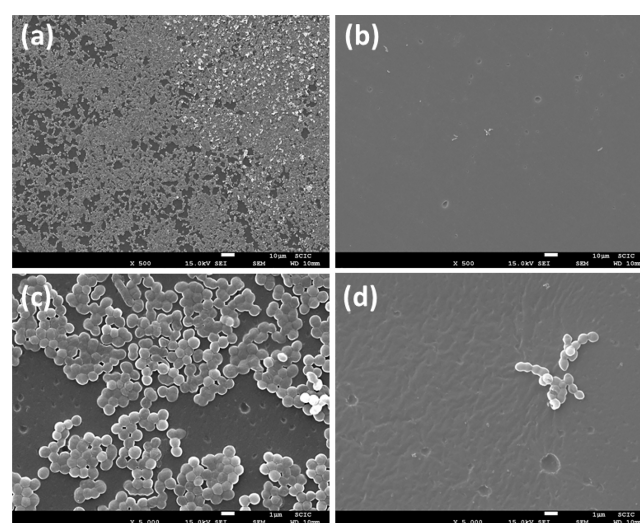


Figure 10. SEM images of hydrogel Mo6@polymer-III with *S. aureus* biofilm, grown in the dark (a and c) and after exposure to light (b and d). Magnification 500× (a, b; scale bar = 10 μm) and 5000× (c, d; scale bar = 1 μm).

show a biofilm formed on the surface of Mo6@polymer-III, at 500× and 5000× magnifications, respectively. Upon irradiation and subsequent washing, the density of bacteria is notably reduced, as can be seen in Figure 10b,d (500× and 5000×, respectively). Since samples were washed before image acquisition, it must be hypothesized that the irradiation weakened the extracellular matrix that holds together the

bacterial biofilm. Additional SEM pictures can be found in Figure S5.

Thus, it can be concluded that the family of molybdenum clusters can be added to the list of photosensitizers successfully used to treat *S. aureus* biofilms, like, for instance, porphyrins⁶⁶ and chlorins,⁶⁷ methylene blue,^{68,69} toluidine blue O,⁷⁰ and hypericin.⁷¹

Regarding the biocidal mechanism, since the phototoxicity of {Mo₆} complexes is related to ¹O₂ production, the photodynamic bactericidal activity against *S. aureus* biofilms could be related to the oxidative damage of this reactive oxygen species. Moreover, it is also known that, in addition to acting directly on bacterial cells, the products generated as a result of irradiations also act on the extracellular matrix of biofilm, increasing the photodynamic efficiency. For instance, Beirão and co-workers have demonstrated a reduction of 81% in the polysaccharide content of the matrix of *P. aeruginosa* biofilms after treatment with a cationic photosensitizer.⁶⁶ In our case, further studies will determine the target of the ¹O₂ generated by **1**.

In summary, three new photoactive materials embedding cluster **1** in different HEMA-based matrixes have been synthesized (radical polymerization initiated by AIBN) and characterized by means of FTIR, TGA, and emission spectroscopy. All the materials display excellent ability to generate ¹O₂ upon irradiation with visible light (400–700 nm), as demonstrated by the reactivity toward two chemical traps (DMA and DHN). Differences have been detected between the photoactive materials, probably attributable to variations in the permeability to solvent and oxygen. Regarding the antimicrobial activity, all the three polyHEMA hydrogels doped with **1** are efficient for inactivation of *S. aureus* biofilms, when irradiated with blue light (460 nm). The material made with the composition of 90% HEMA monomer and 10% PEGDMA cross-linker (**Mo6@polymer-III**) is especially easy to manipulate and achieves the highest levels of bacterial population reductions (3.0 log₁₀ CFU/cm²). The findings here reported open the door for the development, in the future, of new photoactive materials based on other hexanuclear molybdenum cluster photosensitizers and HEMA-based transparent polymeric hydrogels.

EXPERIMENTAL SECTION

HEMA, EGDMA, PEGDMA (M_n 550), and AIBN were purchased from Sigma-Aldrich and used as received. The solvents were spectroscopic grade (Scharlab, S. L.).

Preparation of Photoactive Films. The synthesis of cluster **1** has been described previously in the literature.²⁶ The synthesis of the polymeric sheets is based on previously described procedures.^{50–56} In short, (Bu₄N)₂[Mo₆I₈(CH₃COO)₆] (**1**) was dissolved (1 wt %) in the appropriate mixture of HEMA and EGDMA or PEGDMA, following the proportions detailed in Table 1. Then, AIBN was added and dissolved (1 wt % relative to the total mass of monomer and cross-linker). A small part of this solution was pipetted into the narrow space formed between two microscope glass slides separated by two thin lamellas (100 μm thickness) at the edges. In order to facilitate the later unmolding process, the glass slides were previously treated with silicone oil and cured at 200 °C for 60 min (oven). The system containing the polymerizable mixture was placed in an oven at 85 °C for 15 min. After polymerization, the two glass slides were separated and the film was removed. Finally, the film was washed with distilled water to eliminate any unreacted material.

Steady-State Emission. Steady-state emission of the samples was recorded with an Agilent Cary-Eclipse spectrofluorometer at 25 °C, between 600 and 750 nm, with excitation at 470 nm. The films were

supported between two microscope glass slides and placed on the corresponding solid sample holder to proceed with the measurements.

Fourier-Transform Infrared Spectroscopy (FTIR). FTIR microscopy was performed on a Jasco FT/IR 6200 type A with a TGS detector, between 4000 and 400 cm⁻¹.

Thermogravimetric Analyses (TGA). The thermogravimetric analyses were performed on a TG-SDTA Mettler Toledo model TGA/SDTA851e/LF/1600 coupled to a quadrupole mass spectrometer Pfeiffer Vacuum model Thermostar. The samples (6–7 mg) were heated between 25 and 500 °C, under an air atmosphere, with a heating rate of 10 °C/min.

Scanning Electron Microscopy (SEM). Field-emission scanning electron micrographs were recorded on a JEOL 7001F microscope. The corresponding samples were placed on top of aluminum specimen mount stubs. The samples were then sputtered with Pt (Baltec SCD500) for 30 s and observed at 15 kV.

Benchmark Model Reactions to Test ¹O₂ Production. For the photo-oxygenation reaction of DMA, photochemical reactions were performed inside 10 mL sealed vials containing 50 mg of the polymeric film and 3 mL of an aerated solution of DMA 10⁻⁴ M in EtOH–H₂O (1:1). Irradiations were carried out using two LED lamps (11 W each, Lexman, ca. 400–700 nm emission output) placed 1.5 cm away from the vial during 90 min under continuous stirring. The evolution of the photoreactions was monitored over time by means of UV–vis absorption spectrophotometry (decrease of absorbance at 376 nm).

For the photo-oxygenation reaction of DHN, photochemical reactions were performed inside 10 mL sealed vials containing 50 mg of the polymeric film and 3 mL of an aerated solution of DHN 10⁻⁴ M in DCM–MeOH (9:1). Irradiations were carried out using two LED lamps (11 W each, Lexman, ca. 400–700 nm emission output) placed 4 cm away from the vial during 120 min under continuous stirring. A chemical filter (NaNO₂, 0.72 M solution) between the lamps and the vial was used in this case to minimize the absorption of light by DHN. The evolution of the photoreactions was monitored over time by means of UV–vis absorption spectrophotometry (increase of absorbance at 427 nm and decrease at 300 nm).

Antimicrobial Photodynamic Activity against *S. aureus* Biofilms. *S. aureus* ATCC 29213 (American Type Culture Collection, Rockville, MD) was used to evaluate the antimicrobial photodynamic activity of the {Mo₆} complexes against biofilms. To prepare bacterial inocula (protocol described in the literature^{59–62}), an overnight staphylococcal culture in tryptic soy broth containing 0.25% glucose (TSB) under aerobic conditions at 37 °C using a shaker incubator was adjusted to 0.5 in the McFarland scale (10⁸ cells/mL) and diluted at 1:100 in TSB (final concentration: 10⁶ cells/mL). Each polymeric film containing the photosensitizer (1 cm²) (**Mo6@polymer-I**, **Mo6@polymer-II**, or **Mo6@polymer-III**) and its respective control (**I**, **II**, or **III**) were placed in 6-well flat-bottom tissue culture plates (Cellstar, Greiner bio-one), and 8 mL of inocula was added to each well. The plates were incubated for 24 h at 37 °C for biofilm growth.

At this time, the polymeric films were taken out and washed three times with water to eliminate planktonic cells, and then, they were exposed to light (LED illumination 460 ± 10 nm) for 150 min (fluence 120 J/cm²). Afterward, they were washed with PBS (buffer phosphate saline pH 7.2) and adherent bacteria were detached by sonication (40 kHz, 2 min). The samples were serially diluted in PBS, and viable bacteria were determined by colony counting in Mueller Hinton agar (MHA). The survival bacteria data are expressed as colony-forming unit/cm² (CFU/cm²). In other series of experiments, polymeric films with and without {Mo₆} complexes were not treated with light (dark controls: **Mo6@polymer-I**, **-II**, and **-III** dark and **I**, **II**, and **III** dark).

The bactericidal activity of {Mo₆} complexes against biofilm-forming bacteria was evaluated using the same criterion as that for the bactericidal activity against planktonic bacteria.

All the experiments were performed three times. The results are expressed as mean ± standard deviation. The differences between the

groups were compared by an analysis of variance with statistical significance at $p \leq 0.05$.

For the analysis using SEM, the polymeric films were fixed for 1 h in 2.5% glutaraldehyde and dehydrated in several ethanol washes (10%, 25%, 50%, 75%, and 90% for 20 min and 100% for 1 h). The polymeric samples were dried overnight in a bacteriological incubator at 37 °C, and afterward, they were mounted as described previously.

■ ASSOCIATED CONTENT

Supporting Information

The Supporting Information is available free of charge at <https://pubs.acs.org/doi/10.1021/acsbmaterials.0c00992>.

Figures of irradiation setups, representative polymeric sheet under visible and UV illumination, IR spectra, TGA curves, and SEM images (PDF)

■ AUTHOR INFORMATION

Corresponding Authors

Isabel García-Luque – Departamento de Microbiología, Facultad de Medicina, Universidad de Sevilla, 41009 Sevilla, Spain; Red Española de Investigación en Patología Infecciosa (REIPI RD16/0016/0001), Instituto de Salud Carlos III, 28029 Madrid, Spain; orcid.org/0000-0003-1280-3102; Email: igarcial@us.es

Francisco Galindo – Departamento de Química Inorgánica y Orgánica, Universitat Jaume I, 12071 Castellón, Spain; orcid.org/0000-0003-0826-6084; Email: francisco.galindo@uji.es

Authors

Noelia López-López – Departamento de Química Inorgánica y Orgánica, Universitat Jaume I, 12071 Castellón, Spain; orcid.org/0000-0003-2522-760X

Ignacio Muñoz Resta – Departamento de Química Inorgánica y Orgánica, Universitat Jaume I, 12071 Castellón, Spain

Rosa de Llanos – Unidad Predepartamental de Medicina, Universitat Jaume I, 12071 Castellón, Spain

Juan F. Miravet – Departamento de Química Inorgánica y Orgánica, Universitat Jaume I, 12071 Castellón, Spain; orcid.org/0000-0003-0946-3784

Maxim Mikhaylov – Nikolaev Institute of Inorganic Chemistry, Siberian Branch of the Russian Academy of Sciences, 630090 Novosibirsk, Russia

Maxim N. Sokolov – Nikolaev Institute of Inorganic Chemistry, Siberian Branch of the Russian Academy of Sciences, 630090 Novosibirsk, Russia; orcid.org/0000-0001-9361-4594

Sofía Ballesta – Departamento de Microbiología, Facultad de Medicina, Universidad de Sevilla, 41009 Sevilla, Spain; Red Española de Investigación en Patología Infecciosa (REIPI RD16/0016/0001), Instituto de Salud Carlos III, 28029 Madrid, Spain; orcid.org/0000-0003-3866-6804

Complete contact information is available at:

<https://pubs.acs.org/doi/10.1021/acsbmaterials.0c00992>

Notes

The authors declare no competing financial interest.

■ ACKNOWLEDGMENTS

Ministerio de Ciencia, Innovación y Universidades of Spain (grant RTI2018-101675-B-I00), and Universitat Jaume I (grant UJI-B2018-30) are acknowledged for their financial support. This study was also supported by Plan Nacional de I

+D+i 2013-2016 and Instituto de Salud Carlos III, Subdirección General de Redes y Centros de Investigación Cooperativa, Ministerio de Ciencia, Innovación y Universidades, Spanish Network for Research in Infectious Diseases (REIPI RD16/0016/0001) - cofounded by European Development Regional Fund “A way to achieve Europe”, Operative program Intelligent Growth 2014-2020. I.M.R. would like to thank the Generalitat Valenciana for a Santiago Grisolia fellowship (GRISOLIAP/2018/071). R.d.L. was funded through a Beatriz Galindo Fellowship of the Ministerio de Educación y Formación Profesional, Spanish Government. Technical support from SCIC/UJI is also acknowledged.

■ REFERENCES

- (1) Rice, L. B. Federal Funding for the Study of Antimicrobial Resistance in Nosocomial Pathogens: No ESCAPE. *J. Infect. Dis.* **2008**, *197* (8), 1079–1081.
- (2) Koo, H.; Allan, R. N.; Howlin, R. P.; Stoodley, P.; Hall-Stoodley, L. Targeting Microbial Biofilms: Current and Prospective Therapeutic Strategies. *Nat. Rev. Microbiol.* **2017**, *15* (12), 740–755.
- (3) Lewis, K. Riddle of Biofilm Resistance. *Antimicrob. Agents Chemother.* **2001**, *45* (4), 999–1007.
- (4) Wainwright, M.; Maisch, T.; Nonell, S.; Plaetzer, K.; Almeida, A.; Tegos, G. P.; Hamblin, M. R. Photoantimicrobials—Are We Afraid of the Light? *Lancet Infect. Dis.* **2017**, *17* (2), No. e49.
- (5) Wainwright, M. Synthetic, Small-Molecule Photoantimicrobials - A Realistic Approach. *Photochemical and Photobiological Sciences* **2018**, *17* (11), 1767–1779.
- (6) Cieplik, F.; Deng, D.; Crielaard, W.; Buchalla, W.; Hellwig, E.; Al-Ahmad, A.; Maisch, T. Antimicrobial Photodynamic Therapy—What We Know and What We Don't. *Crit. Rev. Microbiol.* **2018**, *44* (5), 571–589.
- (7) Hamblin, M. R.; Abrahamse, H. Can Light-Based Approaches Overcome Antimicrobial Resistance? *Drug Dev. Res.* **2019**, *80* (1), 48–67.
- (8) Hu, X.; Huang, Y.-Y.; Wang, Y.; Wang, X.; Hamblin, M. R. Antimicrobial Photodynamic Therapy to Control Clinically Relevant Biofilm Infections. *Frontiers in Microbiology* **2018**, *9*, 1–24.
- (9) Jia, Q.; Song, Q.; Li, P.; Huang, W. Rejuvenated Photodynamic Therapy for Bacterial Infections. *Adv. Healthcare Mater.* **2019**, *8*, 1900608.
- (10) Mosinger, J.; Jirsák, O.; Kubát, P.; Lang, K.; Mosinger, B. Bactericidal Nanofabrics Based on Photoproduction of Singlet Oxygen. *J. Mater. Chem.* **2007**, *17* (2), 164–166.
- (11) Feese, E.; Sadeghifar, H.; Gracz, H. S.; Argyropoulos, D. S.; Ghiladi, R. A. Photobactericidal Porphyrin-Cellulose Nanocrystals: Synthesis, Characterization, and Antimicrobial Properties. *Biomacromolecules* **2011**, *12* (10), 3528–3539.
- (12) Benabbou, A. K.; Guillard, C.; Pigeot-Rémy, S.; Cantau, C.; Pigot, T.; Lejeune, P.; Derriche, Z.; Lacombe, S. Water Disinfection Using Photosensitizers Supported on Silica. *J. Photochem. Photobiol., A* **2011**, *219* (1), 101–108.
- (13) Rahal, R.; Le Behec, M.; Guyoneaud, R.; Pigot, T.; Paolacci, H.; Lacombe, S. Bactericidal Activity under UV and Visible Light of Cotton Fabrics Coated with Anthraquinone-Sensitized TiO₂. *Catal. Today* **2013**, *209*, 134–139.
- (14) Henke, P.; Kozak, H.; Artemenko, A.; Kubat, P.; Forstova, J.; Mosinger, J. Superhydrophilic Polystyrene Nanofiber Materials Generating O₂(¹Δ_g): Postprocessing Surface Modifications toward Efficient Antibacterial Effect. *ACS Appl. Mater. Interfaces* **2014**, *6*, 13007–13014.
- (15) Noimark, S.; Weiner, J.; Noor, N.; Allan, E.; Williams, C. K.; Shaffer, M. S. P.; Parkin, I. P. Dual-Mechanism Antimicrobial Polymer-ZnO Nanoparticle and Crystal Violet-Encapsulated Silicone. *Adv. Funct. Mater.* **2015**, *25* (9), 1367–1373.
- (16) Sehmi, S. K.; Noimark, S.; Bear, J. C.; Peveler, W. J.; Bovis, M.; Allan, E.; MacRobert, A. J.; Parkin, I. P. Lethal Photosensitisation of Staphylococcus Aureus and Escherichia Coli Using Crystal Violet and

Zinc Oxide-Encapsulated Polyurethane. *J. Mater. Chem. B* **2015**, *3* (31), 6490–6500.

(17) Spagnul, C.; Turner, L. C.; Boyle, R. W. Immobilized Photosensitizers for Antimicrobial Applications. *J. Photochem. Photobiol., B* **2015**, *150*, 11–30.

(18) Abrahamse, H. R.; Hamblin, M. R. New photosensitizers for photodynamic therapy. *Biochem. J.* **2016**, *473*, 347–364.

(19) Maverick, A. W.; Najdzionek, J. S.; MacKenzie, D.; Nocera, D. G.; Gray, H. B. Spectroscopic, Electrochemical, and Photochemical Properties of Molybdenum(II) and Tungsten(II) Halide Clusters. *J. Am. Chem. Soc.* **1983**, *105* (7), 1878–1882.

(20) Grasset, F.; Molard, Y.; Cordier, S.; Dorson, F.; Mortier, M.; Perrin, C.; Guilloux-Viry, M.; Sasaki, T.; Haneda, H. When “Metal Atom Clusters” Meet ZnO Nanocrystals: A $((n-C_4H_9)_4N)_2Mo_6Br_{14}@ZnO$ Hybrid. *Adv. Mater.* **2008**, *20* (9), 1710–1715.

(21) Molard, Y.; Dorson, F.; Circu, V.; Roisnel, T.; Artzner, F.; Cordier, S. Clustomesogens: Liquid Crystal Materials Containing Transition-Metal Clusters. *Angew. Chem., Int. Ed.* **2010**, *49* (19), 3351–3355.

(22) Sokolov, M. N.; Mihailov, M. A.; Peresyphkina, E. V.; Brylev, K. A.; Kitamura, N.; Fedin, V. P. Highly Luminescent Complexes $[Mo_6X_8(n-C_3F_7COO)_6]^{2-}$ ($X = Br, I$). *Dalton Transactions* **2011**, *40* (24), 6375–6377.

(23) Kirakci, K.; Kubát, P.; Dušek, M.; Fejfarová, K.; Šícha, V.; Mosinger, J.; Lang, K. A Highly Luminescent Hexanuclear Molybdenum Cluster - A Promising Candidate toward Photoactive Materials. *Eur. J. Inorg. Chem.* **2012**, *2012* (19), 3107–3111.

(24) Sokolov, M. N.; Mikhailov, M. A.; Brylev, K. A.; Virovets, A. V.; Vicent, C.; Kompankov, N. B.; Kitamura, N.; Fedin, V. P. Alkynyl Complexes of High-Valence Clusters. Synthesis and Luminescence Properties of $[Mo_6I_8(C\equiv CC(O)OMe)_6]^{2-}$, the First Complex with Exclusively Organometallic Outer Ligands in the Family of Octahedral $\{M_6X_8\}$ Clusters. *Inorg. Chem.* **2013**, *52* (21), 12477–12481.

(25) Efremova, O. A.; Vorotnikov, Y. A.; Brylev, K. A.; Vorotnikova, N. A.; Novozhilov, I. N.; Kuratieva, N. V.; Edeleva, M. V.; Benoit, D. M.; Kitamura, N.; Mironov, Y. V.; Shestopalov, M. A.; Sutherland, A. J. Octahedral Molybdenum Cluster Complexes with Aromatic Sulfonate Ligands. *Dalton Transactions* **2016**, *45* (39), 15427–15435.

(26) Mikhailov, M. A.; Brylev, K. A.; Abramov, P. A.; Sakuda, E.; Akagi, S.; Ito, A.; Kitamura, N.; Sokolov, M. N. Synthetic Tuning of Redox, Spectroscopic, and Photophysical Properties of $\{Mo_6I_8\}^{4+}$ Core Cluster Complexes by Terminal Carboxylate Ligands. *Inorg. Chem.* **2016**, *55* (17), 8437–8445.

(27) Mikhailov, M. A.; Brylev, K. A.; Virovets, A. V.; Gallyamov, M. R.; Novozhilov, I.; Sokolov, M. N. Complexes of $\{Mo_6I_8\}$ with Nitrophenolates: Synthesis and Luminescence. *New J. Chem.* **2016**, *40* (2), 1162–1168.

(28) Evtushok, D. V.; Melnikov, A. R.; Vorotnikova, N. A.; Vorotnikov, Y. A.; Ryadun, A. A.; Kuratieva, N. V.; Kozyr, K. V.; Obedinskaya, N. R.; Kretov, E. I.; Novozhilov, I. N.; Mironov, Y. V.; Stass, D. V.; Efremova, O. A.; Shestopalov, M. A. A Comparative Study of Optical Properties and X-Ray Induced Luminescence of Octahedral Molybdenum and Tungsten Cluster Complexes. *Dalton Transactions* **2017**, *46* (35), 11738–11747.

(29) Volostnykh, M. V.; Mikhaylov, M. A.; Sinelshchikova, A. A.; Kirakosyan, G. A.; Martynov, A. G.; Grigoriev, M. S.; Piryazev, D. A.; Tsvadze, A. Y.; Sokolov, M. N.; Gorbunova, Y. G. Hybrid Organic-Inorganic Supramolecular Systems Based on a Pyridine End-Decorated Molybdenum(II) Halide Cluster and Zinc(II) Porphyrinate. *Dalton Transactions* **2019**, *48* (5), 1835–1842.

(30) Fabre, B.; Cordier, S.; Molard, Y.; Perrin, C.; Ababou-Girard, S.; Godet, C. Electrochemical and Charge Transport Behavior of Molybdenum-Based Metallic Cluster Layers Immobilized on Modified n- and p-Type Si(111) Surfaces. *J. Phys. Chem. C* **2009**, *113* (40), 17437–17446.

(31) Molard, Y.; Labbé, C.; Cardin, J.; Cordier, S. Sensitization of Er^{3+} Infrared Photoluminescence Embedded in a Hybrid Organic-

Inorganic Copolymer Containing Octahedral Molybdenum Clusters. *Adv. Funct. Mater.* **2013**, *23* (38), 4821–4825.

(32) Aubert, T.; Cabello-Hurtado, F.; Esnault, M. A.; Neaime, C.; Lebret-Chauvel, D.; Jeanne, S.; Pellen, P.; Roiland, C.; Le Polles, L.; Saito, N.; Kimoto, K.; Haneda, H.; Ohashi, N.; Grasset, F.; Cordier, S. Extended Investigations on Luminescent $CS_2[Mo_6Br_{14}]@SiO_2$ Nanoparticles: Physico-Structural Characterizations and Toxicity Studies. *J. Phys. Chem. C* **2013**, *117* (39), 20154–20163.

(33) Amela-Cortes, M.; Garreau, A.; Cordier, S.; Faulques, E.; Duval, J. L.; Molard, Y. Deep Red Luminescent Hybrid Copolymer Materials with High Transition Metal Cluster Content. *J. Mater. Chem. C* **2014**, *2* (8), 1545–1552.

(34) Efremova, O. A.; Shestopalov, M. A.; Chirtsova, N. A.; Smolentsev, A. I.; Mironov, Y. V.; Kitamura, N.; Brylev, K. A.; Sutherland, A. J. A Highly Emissive Inorganic Hexamolybdenum Cluster Complex as a Handy Precursor for the Preparation of New Luminescent Materials. *Dalton Transactions* **2014**, *43* (16), 6021–6025.

(35) Kirakci, K.; Šícha, V.; Holub, J.; Kubát, P.; Lang, K. Luminescent Hydrogel Particles Prepared by Self-Assembly of β -Cyclodextrin Polymer and Octahedral Molybdenum Cluster Complexes. *Inorg. Chem.* **2014**, *53* (24), 13012–13018.

(36) Amela-Cortes, M.; Paofai, S.; Cordier, S.; Folliot, H.; Molard, Y. Tuned Red NIR Phosphorescence of Polyurethane Hybrid Composites Embedding Metallic Nanoclusters for Oxygen Sensing. *Chem. Commun.* **2015**, *51* (38), 8177–8180.

(37) Amela-Cortes, M.; Molard, Y.; Paofai, S.; Desert, A.; Duval, J. L.; Naumov, N. G.; Cordier, S. Versatility of the Ionic Assembling Method to Design Highly Luminescent PMMA Nanocomposites Containing $[M_6Q_8L_6]^{n-}$ Octahedral Nano-Building Blocks. *Dalton Transactions* **2016**, *45* (1), 237–245.

(38) Neaime, C.; Amela-Cortes, M.; Grasset, F.; Molard, Y.; Cordier, S.; Dierre, B.; Mortier, M.; Takei, T.; Takahashi, K.; Haneda, H.; Verelst, M.; Lechevallier, S. Time-Gated Luminescence Bioimaging with New Luminescent Nanocolloids Based on $[Mo_6I_8(C_2F_5COO)_6]^{2-}$ Metal Atom Clusters. *Phys. Chem. Chem. Phys.* **2016**, *18* (43), 30166–30173.

(39) Kirakci, K.; Kubát, P.; Fejfarová, K.; Martinčík, J.; Nikl, M.; Lang, K. X-Ray Inducible Luminescence and Singlet Oxygen Sensitization by an Octahedral Molybdenum Cluster Compound: A New Class of Nanoscintillators. *Inorg. Chem.* **2016**, *55* (2), 803–809.

(40) Solovieva, A. O.; Vorotnikov, Y. A.; Trifonova, K. E.; Efremova, O. A.; Krasilnikova, A. A.; Brylev, K. A.; Vorontsova, E. V.; Avrorov, P. A.; Shestopalova, L. V.; Poveshchenko, A. F.; Mironov, Y. V.; Shestopalov, M. A. Cellular Internalisation, Bioimaging and Dark and Photodynamic Cytotoxicity of Silica Nanoparticles Doped by $\{Mo_6I_8\}^{4+}$ Metal Clusters. *J. Mater. Chem. B* **2016**, *4* (28), 4839–4846.

(41) Efremova, O. A.; Brylev, K. A.; Vorotnikov, Y. A.; Vejsadová, L.; Shestopalov, M. A.; Chimonides, G. F.; Mikes, P.; Topham, P. D.; Kim, S. J.; Kitamura, N.; Sutherland, A. J. Photoluminescent Materials Based on PMMA and a Highly-Emissive Octahedral Molybdenum Metal Cluster Complex. *J. Mater. Chem. C* **2016**, *4* (3), 497–503.

(42) Elistratova, J.; Mukhametshina, A.; Kholin, K.; Nizameev, I.; Mikhailov, M.; Sokolov, M.; Khairullin, R.; Miftakhova, R.; Shammass, G.; Kadirov, M.; Petrov, K.; Rizvanov, A.; Mustafina, A. Interfacial Uploading of Luminescent Hexamolybdenum Cluster Units onto Amino-Decorated Silica Nanoparticles as New Design of Nanomaterial for Cellular Imaging and Photodynamic Therapy. *J. Colloid Interface Sci.* **2019**, *538*, 387–396.

(43) Arnau del Valle, C.; Felip-León, C.; Angulo-Pachón, C. A.; Mikhailov, M.; Sokolov, M. N.; Miravet, J. F.; Galindo, F. Photoactive Hexanuclear Molybdenum Nanoclusters Embedded in Molecular Organogels. *Inorg. Chem.* **2019**, *58* (14), 8900–8905.

(44) Ghogare, A. A.; Greer, A. Using Singlet Oxygen to Synthesize Natural Products and Drugs. *Chem. Rev.* **2016**, *116* (17), 9994–10034.

(45) Fabregat, V.; Burguete, M. I.; Luis, S. V.; Galindo, F. Improving Photocatalytic Oxygenation Mediated by Polymer Supported Photo-

sensitizers Using Semiconductor Quantum Dots as “Light Antennas.” *RSC Adv.* **2017**, *7* (56), 35154–35158.

(46) Beltrán, A.; Mikhailov, M.; Sokolov, M. N.; Pérez-Laguna, V.; Rezusta, A.; Revillo, M. J.; Galindo, F. A Photobleaching Resistant Polymer Supported Hexanuclear Molybdenum Iodide Cluster for Photocatalytic Oxygenations and Photodynamic Inactivation of: *Staphylococcus Aureus*. *J. Mater. Chem. B* **2016**, *4* (36), 5975–5979.

(47) Felip-León, C.; Arnau Del Valle, C.; Pérez-Laguna, V.; Isabel Millán-Lou, M.; Miravet, J. F.; Mikhailov, M.; Sokolov, M. N.; Rezusta-López, A.; Galindo, F. Superior Performance of Macroporous over Gel Type Polystyrene as a Support for the Development of Photo-Bactericidal Materials. *J. Mater. Chem. B* **2017**, *5* (30), 6058–6064.

(48) Kirakci, K.; Zelenka, J.; Rumlová, M.; Cvačka, J.; Ruml, T.; Lang, K. Cationic Octahedral Molybdenum Cluster Complexes Functionalized with Mitochondria-Targeting Ligands: Photodynamic Anticancer and Antibacterial Activities. *Biomater. Sci.* **2019**, *7* (4), 1386–1392.

(49) Vorotnikova, N. A.; Alekseev, A. Y.; Vorotnikov, Y. A.; Evtushok, D. V.; Molard, Y.; Amela-Cortes, M.; Cordier, S.; Smolentsev, A. I.; Burton, C. G.; Kozhin, P. M.; Zhu, P.; Topham, P. D.; Mironov, Y. V.; Bradley, M.; Efremova, O. A.; Shestopalov, M. A. Octahedral Molybdenum Cluster as a Photoactive Antimicrobial Additive to a Fluoroplastic. *Mater. Sci. Eng., C* **2019**, *105*, 110150.

(50) Galindo, F.; Lima, J. C.; Luis, S. V.; Parola, A. J.; Pina, F. Write-Read-Erase Molecular-Switching System Trapped in a Polymer Hydrogel Matrix. *Adv. Funct. Mater.* **2005**, *15* (4), 541–545.

(51) Galindo, F.; Lima, J. C.; Luis, S. V.; Melo, M. J.; Parola, A. J.; Pina, F. Water/Humidity and Ammonia Sensor, Based on a Polymer Hydrogel Matrix Containing a Fluorescent Flavylum Compound. *J. Mater. Chem.* **2005**, *15* (27–28), 2840–2847.

(52) Bru, M.; Burguete, M. I.; Galindo, F.; Luis, S. V.; Marín, M. J.; Vigara, L. Cross-Linked Poly(2-hydroxyethylmethacrylate) Films Doped with 1,2-Diaminoanthraquinone (DAQ) as Efficient Materials for the Colorimetric Sensing of Nitric Oxide and Nitrite Anion. *Tetrahedron Lett.* **2006**, *47* (11), 1787–1791.

(53) Burguete, M. I.; Fabregat, V.; Galindo, F.; Izquierdo, M. A.; Luis, S. V. Improved Poly HEMA-DAQ Films for the Optical Analysis of Nitrite. *Eur. Polym. J.* **2009**, *45* (5), 1516–1523.

(54) Fabregat, V.; Izquierdo, M. A.; Burguete, M. I.; Galindo, F.; Luis, S. V. Quantum Dot-Polymethacrylate Composites for the Analysis of NO_x by Fluorescence Spectroscopy. *Inorg. Chim. Acta* **2012**, *381* (1), 212–217.

(55) Fabregat, V.; Izquierdo, M. A.; Burguete, M. I.; Galindo, F.; Luis, S. V. Nitric Oxide Sensitive Fluorescent Polymeric Hydrogels Showing Negligible Interference by Dehydroascorbic Acid. *Eur. Polym. J.* **2014**, *55* (1), 108–113.

(56) Fabregat, V.; Burguete, M. I.; Galindo, F.; Luis, S. V. Influence of Polymer Composition on the Sensitivity towards Nitrite and Nitric Oxide of Colorimetric Disposable Test Strips. *Environ. Sci. Pollut. Res.* **2017**, *24* (4), 3448–3455.

(57) Atzet, S.; Curtin, S.; Trinh, P.; Bryant, S.; Ratner, B. Degradable Poly(2-hydroxyethyl Methacrylate)-Co-Polycaprolactone Hydrogels for Tissue Engineering Scaffolds. *Biomacromolecules* **2008**, *9* (12), 3370–3377.

(58) Galperin, A.; Smith, K.; Geisler, N. S.; Bryers, J. D.; Ratner, B. D. Precision-Porous Poly HEMA-Based Scaffold as an Antibiotic-Releasing Insert for a Scleral Bandage. *ACS Biomater. Sci. Eng.* **2015**, *1* (7), 593–600.

(59) de Melo, W. C. M. A.; Avci, P.; de Oliveira, M. N.; Gupta, A.; Vecchio, D.; Sadasivam, M.; Chandran, R.; Huang, Y. Y.; Yin, R.; Perussi, L. R.; Tegos, G. P.; Perussi, J. R.; Dai, T.; Hamblin, M. R. Photodynamic Inactivation of Biofilm: Taking a Lightly Colored Approach to Stubborn Infection. *Expert Rev. Anti-Infect. Ther.* **2013**, *11* (7), 669–693.

(60) García, I.; Ballesta, S.; Gilaberte, Y.; Rezusta, A.; Pascual, A. Antimicrobial photodynamic activity of hypericin against methicillin-susceptible and resistant *Staphylococcus aureus* biofilms. *Future Microbiol.* **2015**, *10*, 347–356.

(61) Pérez-Laguna, V.; Pérez-Artiaga, L.; Lampaya-Pérez, V.; García-Luque, I.; Ballesta, S.; Nonell, S.; Paz-Cristobal, M. P.; Gilaberte, Y.; Rezusta, A. Bactericidal Effect of Photodynamic Therapy, Alone or in Combination with Mupirocin or Linezolid, on *Staphylococcus aureus*. *Front. Microbiol.* **2017**, *8*, 1002.

(62) Pérez-Laguna, V.; García-Luque, I.; Ballesta, S.; Pérez-Artiaga, L.; Lampaya-Pérez, V.; Samper, S.; Soria-Lozano, P.; Rezusta, A.; Gilaberte, Y. Antimicrobial photodynamic activity of Rose Bengal, alone or in combination with Gentamicin, against planktonic and biofilm *Staphylococcus aureus*. *Photodiagn. Photodyn. Ther.* **2018**, *21*, 211–216.

(63) Bankier, C.; Cheong, Y.; Mahalingam, S.; Edirisinghe, M.; Ren, G.; Cloutman-Green, E.; Ciric, L. A comparison of methods to assess the antimicrobial activity of nanoparticle combinations on bacterial cells. *PLoS One* **2018**, *13* (2), No. e0192093.

(64) *Performance Standards for Antimicrobial Susceptibility Testing, CLSI M100*, 28th ed.; Clinical and Laboratory Standards Institute: Wayne, PA, 2013.

(65) Dai, T.; Gupta, A.; Murray, C. K.; Vrahas, M. S.; Tegos, G. P.; Hamblin, M. R. Blue Light for Infectious Diseases: Propionibacterium Acnes, Helicobacter Pylori, and Beyond? *Drug Resist. Updates* **2012**, *15* (4), 223–236.

(66) Beirão, S.; Fernandes, S.; Coelho, J.; Faustino, M. A. F.; Tomé, J. P. C.; Neves, M. G. P. M. S.; Tomé, A. C.; Almeida, A.; Cunha, A. Photodynamic Inactivation of Bacterial and Yeast Biofilms with a Cationic Porphyrin. *Photochem. Photobiol.* **2014**, *90* (6), 1387–1396.

(67) Dai, T.; Tegos, G. P.; Zhiyentayev, T.; Mylonakis, E.; Hamblin, M. R. Photodynamic Therapy for Methicillin-Resistant *Staphylococcus Aureus* Infection in a Mouse Skin Abrasion Model. *Lasers Surg. Med.* **2010**, *42* (1), 38.

(68) Pereira, C. A.; Romeiro, R. L.; Costa, A. C. B. P.; MacHado, A. K. S.; Junqueira, J. C.; Jorge, A. O. C. Susceptibility of *Candida Albicans*, *Staphylococcus Aureus*, and *Streptococcus Mutans* Biofilms to Photodynamic Inactivation: An in Vitro Study. *Lasers in Medical Science* **2011**, *26* (3), 341–348.

(69) Gad, F.; Zahra, T.; Hasan, T.; Hamblin, M. R. Effects of Growth Phase and Extracellular Slime on Photodynamic Inactivation of Gram-Positive Pathogenic Bacteria. *Antimicrob. Agents Chemother.* **2004**, *48* (6), 2173–2178.

(70) Sharma, M.; Visai, L.; Bragheri, F.; Cristiani, I.; Gupta, P. K.; Speziale, P. Toluidine Blue-Mediated Photodynamic Effects on *Staphylococcal* Biofilms. *Antimicrob. Agents Chemother.* **2008**, *52* (1), 299–305.

(71) Engelhardt, V.; Krammer, B.; Plaetzer, K. Antibacterial Photodynamic Therapy Using Water-Soluble Formulations of Hypericin or MTHPC Is Effective in Inactivation of *Staphylococcus Aureus*. *Photochemical and Photobiological Sciences* **2010**, *9* (3), 365–369.